Global geometric indicator of chaos and Lyapunov exponents in Hamiltonian systems

K. Ramasubramanian and M. S. Sriram*
Department of Theoretical Physics, University of Madras, Guindy Campus, Chennai 600 025, India
(Received 11 October 2000; revised manuscript received 9 May 2001; published 20 September 2001)

Recently a geometric description of chaos in Hamiltonian systems has been formulated using the tools of Riemannian geometry. Here, Hamiltonian chaos is explained in terms of the curvature properties of the configuration space manifold. In particular, it has been claimed that the average of an appropriately defined sectional curvature ($K^{(2)}$) over a constant energy manifold is a measure of the global extent of chaoticity for systems with a small number of degrees of freedom. We investigate the relations between this quantity $K^{(2)}$ and the maximal Lyapunov exponent λ for some Hamiltonian systems of physical interest with two degrees of freedom. We find that there is a close relation between $K^{(2)}$ and λ^2. Both the quantities scale as $E^{1/2}$ for quartic potentials, where E is the energy. They are expected to scale as $E^{(n-2)/n}$ for a general potential of degree n. However, we find that though $K^{(2)}$ is a global indicator of chaos, it is not a sufficiently accurate measure of order-chaos transitions, in all cases.

DOI: 10.1103/PhysRevE.64.046207 PACS number(s): 05.45.−a, 45.05.+x, 02.60.Cb

I. INTRODUCTION

Recently a geometric approach has been developed to explain the origin of chaos in Hamiltonian systems [1–5]. This approach exploits the fact that the trajectories of a Hamiltonian system can be viewed as geodesics on a Riemannian manifold endowed with a suitable metric.

Consider a dynamical system described by the Lagrangian,

$$L(\mathbf{q},\dot{\mathbf{q}})=\tfrac{1}{2}a_{ik}(\mathbf{q})\dot{q}^i\dot{q}^k-V(\mathbf{q}), \tag{1}$$

or equivalently the Hamiltonian,

$$H(\mathbf{p},\mathbf{q})=\tfrac{1}{2}a^{ik}(\mathbf{q})p_ip_k+V(\mathbf{q}). \tag{2}$$

For a fixed energy E, define the metric tensor

$$g_{ij}=(E-V)a_{ij}, \tag{3}$$

and the ''interval'' or the ''proper time'' ds by

$$ds^2=g_{ij}dq^idq^j=2(E-V)^2dt^2. \tag{4}$$

It can then be shown that the equations of motion can be written as geodesic equations in a Riemannian manifold,

$$\frac{d^2q^i}{ds^2}+\Gamma^i_{jk}\frac{dq^i}{ds}\frac{dq^k}{ds}=0, \tag{5}$$

where Γ^i_{jk} are the Christoffel symbols associated with g_{ij}.

Further, the Jacobi-Levi-Civita equation for the geodesic spread [6] is essentially the tangent flow equations in the geometric form [1],

$$\frac{\nabla}{ds}\left(\frac{\nabla J^i}{ds}\right)+\left(R^i_{jkl}J^k\frac{dq^l}{ds}\right)\frac{dq^j}{ds}=0, \tag{6}$$

where $J^i=\delta q^i$ denotes the tangent vector, $\nabla/(ds)$ is the covariant derivative along a geodesic, and R^i_{jkl} is the Riemann curvature tensor.

Pettini and co-workers [1–5] have shown that the dominant source of chaos in Hamiltonian flows of physical interest is the parametric resonance induced by fluctuations of the scalar curvature even in regions where the curvature is mostly positive. This is true of systems with small as well as large number of degrees of freedom. This approach is different from the geometric description of chaos in abstract ergodic theory, where chaos arises due to the negativeness of the curvature of the manifold. More recently, a local geometric indicator of chaos for single orbits in the Henon-Heiles Hamiltonian system has been formulated by casting the dynamics as a geodesic flow on a Finsler manifold [7]. This gives a one-to-one correspondence between geometry and instability and helps to discriminate between regular and stochastic orbits on a given energy surface.

The geometric approach to chaos has another attractive feature. For systems with a large number of degrees of freedom (N), it has been shown that the ''global degree of chaoticity'' can be obtained by computing the mean Ricci curvature averaged over a constant energy manifold, independent of the dynamics of the system [2]. It is possible to obtain an analytic estimate of the largest Lyapunov exponent λ, by making a Gaussian hypothesis about the statistics of curvature fluctuations along a geodesic. This exponent is in very good agreement with the corresponding exponent obtained from tangent dynamics [3]. Moreover, it has been demonstrated that the geometric approach can even provide a framework for understanding phase transitions that are related to the singular behavior of curvature fluctuations [5]. When the number of degrees of freedom is small, one has to take recourse to other methods as the Gaussian hypothesis is untenable. It has been proposed that the average of a suitable negative sectional curvature (to be defined in the next section) over a constant energy manifold, is a global indicator of chaos for Hamiltonian systems with two degrees of freedom [4]; this has been verified in the case of the Hénon-Heiles model. In this paper, we explore the relation between this

*Email address: tphysmu@satyam.net.in

geometric quantity and the Lyapunov exponent for some Hamiltonians of physical interest and examine the veracity of this claim.

II. SECTIONAL CURVATURE AS A GLOBAL MEASURE OF CHAOS

By simple algebraic manipulations of Eq. (6), it can be shown that

$$\frac{1}{2}\frac{d^2}{ds^2}\|\mathbf{J}\|^2+K^{(2)}(\mathbf{J},\mathbf{v})\|\mathbf{J}\|^2-\left\|\frac{\nabla}{ds}\mathbf{J}\right\|^2=0, \tag{7}$$

where

$$\|\mathbf{J}\|^2=g_{ij}J^iJ^j, \tag{8}$$

$$v^i=\frac{dq^i}{ds}, \quad \text{with } \langle \mathbf{J},\mathbf{v}\rangle=g_{ij}J^iv^j=0, \tag{9}$$

and $K^{(2)}(\mathbf{J},\mathbf{v})$ is the sectional curvature given by

$$K^{(2)}(\mathbf{J},\mathbf{v})=R_{\mu\nu\lambda\eta}\frac{J^\mu}{\|J\|}\frac{dq^\nu}{ds}\frac{J^\eta}{\|J\|}\frac{dq^\lambda}{ds}. \tag{10}$$

It is obvious from Eq. (7) that any point with $K^{(2)}<0$ is an unstable point. Hence it is expected that the average of $K^{(2)}$ over those points in the manifold where it is negative, will give information about the degree of chaos for that manifold.

It has been argued that it is necessary to go to a higher dimensional manifold by augmenting the configuration space, to get reliable information about the degree of chaos in the system [1,4]. It turns out that an enlarged configuration space equipped with the Eisenhart metric [8] is well suited for the purpose. The local coordinates of the enlarged manifold are $q^0,q^1,\ldots,q^N,q^{N+1}$ where $q^1,\ldots,q^N$ are the coordinates of the systems, $q^0=t$ is the time coordinate, and q^{N+1} is an extra coordinate related to the action. The Eisenhart metric $(g_E)_{\mu\nu}$ is defined through the relation

$$ds_E^2=(g_E)_{\mu\nu}dq^\mu dq^\nu=a_{ij}dq^idq^j-2V(\mathbf{q})(dq^0)^2+2dq^0dq^{N+1}, \tag{11}$$

where $\mu,\nu=0,1,\ldots,N+1$, $i,j,=1,\ldots,N$, and a_{ij} is the kinetic energy matrix. When $a_{ij}=\delta_{ij}$, it can be shown that the geodesic equation leads to the equations of motion when

$$ds_E^2=2c_1^2dt^2, q^{N+1}(t)=c_1^2t+c_2-\int_0^t L(\mathbf{q},\dot{\mathbf{q}})dt, \tag{12}$$

c_1,c_2 being arbitrary constants. Further, the only nonvanishing Christoffel coefficients in this case are

$$\Gamma^i_{00}=\partial^iV, \quad \Gamma^{N+1}_{0i}=-\partial_iV, \tag{13}$$

and the nonvanishing components of the Riemann tensor are

$$R_{0i0j}=\frac{\partial^2V}{\partial q^i\partial q^j}. \tag{14}$$

The sectional curvature $K^{(2)}(\mathbf{J},\mathbf{v})$ depends upon the choice of $\mathbf{J}$. For a system with two degrees of freedom, a simple choice is $\mathbf{J}=(J_0=0,J_1=\dot{q}_2,J_2=-\dot{q}_1,J_3=0)$. This choice satisfies $\langle\mathbf{J},\mathbf{v}\rangle=0$. Corresponding to this choice, the sectional curvature for a system with two degrees of freedom can be shown to be

$$K^{(2)}(\dot{\mathbf{q}},\mathbf{q})=\frac{1}{2(E-V)}\left[\frac{\partial^2V}{\partial q_1^2}\dot{q}_2^2+\frac{\partial^2V}{\partial q_2^2}\dot{q}_1^2-2\frac{\partial^2V}{\partial q_1\partial q_2}\dot{q}_1\dot{q}_2\right]. \tag{15}$$

$\langle K_-^{(2)}\rangle$ is the average of the negative values assumed by the sectional curvature over a constant energy surface Σ_E, and is given by

$$\langle K_-^{(2)}\rangle=\frac{1}{A(\Sigma_E)}\int_{\Sigma_E}d\sigma_E K_-^{(2)}=\frac{1}{A(\Sigma_E)}\int d\mathbf{p}d\mathbf{q}\,\delta(H(\mathbf{p},\mathbf{q})-E)\Theta(-K^{(2)})K^{(2)}(\mathbf{p},\mathbf{q}), \tag{16}$$

where the area $A(\Sigma_E)$ is given by

$$A(\Sigma_E)=\int_{\Sigma_E}d\sigma_E=\int d\mathbf{p}d\mathbf{q}\,\delta(H(\mathbf{p},\mathbf{q})-E), \tag{17}$$

and Θ is the step function. This quantity $\langle K_-^{(2)}\rangle$ is the object of central interest in this paper.

It has been shown in the case of the Hénon-Heiles system, that there is a close correspondence between $\langle K_-^{(2)}\rangle$ and the fraction of phase space that is chaotic (obtained by computing the maximal Lyapunov exponent λ for a large number of initial conditions). In particular, in this system $\langle K_-^{(2)}\rangle$ gives a correct estimate of the transition from order to chaos, when the energy is varied.

We make a detailed comparison between $\langle K_-^{(2)}\rangle$ and λ for the following two systems with two degrees of freedom.

(1) Coupled quartic oscillator (CQO):

$$H=\frac{p_1^2}{2}+\frac{p_1^2}{2}+q_1^4+q_2^4+\alpha q_1^2q_2^2, \tag{18}$$

where α is a parameter. This system with a homogeneous quartic potential, is known to be integrable for $\alpha=0$, 2, and 6 and certainly nonintegrable for higher values of α. By way of illustration, we give the Poincare surfaces of section corresponding to the integrable ($\alpha=6$) and nonintegrable ($\alpha=15$) cases in Fig. 1. The Hamiltonian in Eq. (18) finds several applications, particularly in high-energy physics [9].

(2) Yang-Mills-Higgs (YMH) Hamiltonian:

$$H=\frac{p_1^2}{2}+\frac{p_1^2}{2}+3q_1^2q_2^2+\frac{3}{4}q_1^4+\frac{3}{2}\kappa q_2^4-\frac{1}{2}\kappa q_2^2. \tag{19}$$

This is the dynamical system corresponding to the Yang-Mills-Higgs field theory that is of great physical interest in high-energy physics, when spatially homogeneous fields are considered and a suitable ansatz for the fields is employed [10,11]. Here κ is a parameter.

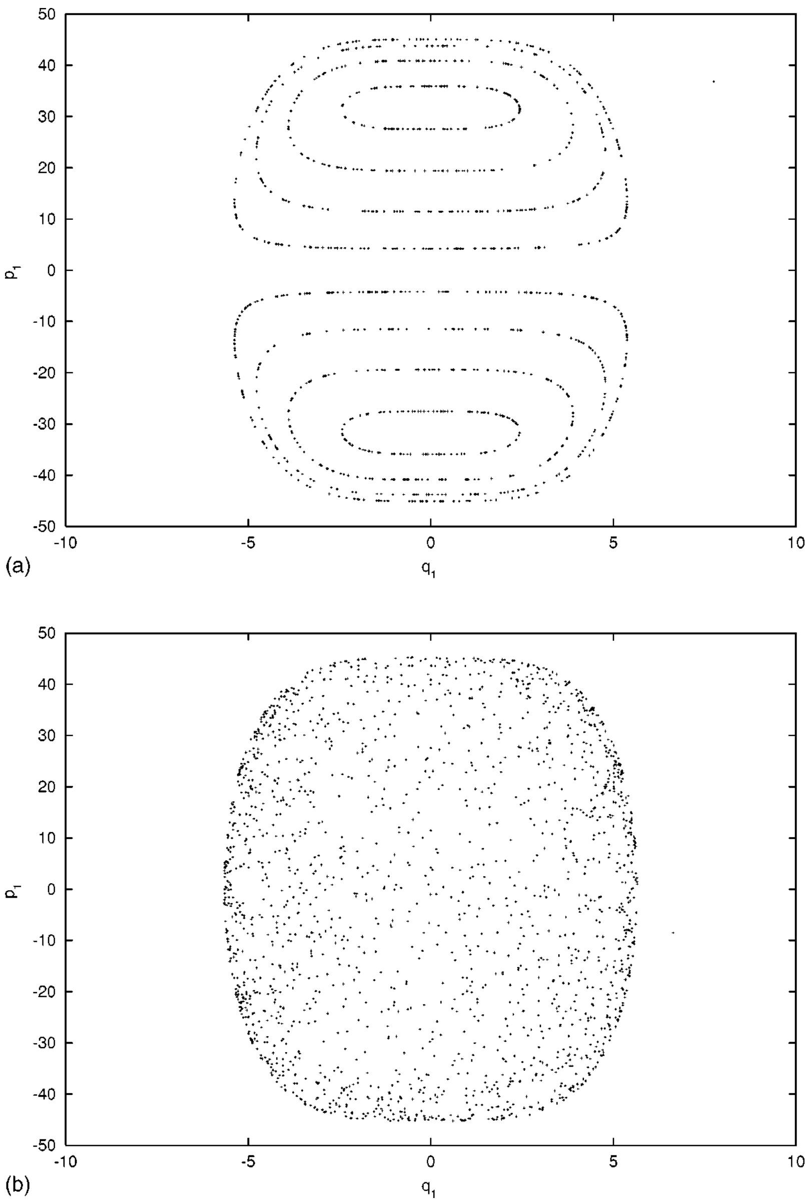

FIG. 1. Typical Poincaré surfaces of section corresponding to (a) the integrable ($\alpha=6$) and (b) nonintegrable ($\alpha=15$) cases at energy $E=1024$, for the system of coupled quartic oscillators.

A constant energy manifold is covered by ''regular islands'' for which λ is zero, surrounded by ''chaotic regions'' corresponding to which λ is a positive number. For specified values of the energy E and the parameter of the system (α or κ), λ is computed for a large number of randomly chosen initial conditions to determine the average value of λ and the fraction of the phase space f, corresponding to chaotic trajectories. f is simply the fraction of the number of initial conditions for which λ is a positive quantity. An integration time $\sim 10\,000$ units was sufficient to ensure convergence of λ, in all the cases we considered. The numerically computed value of λ is not exactly zero on finite time scales, even for regular trajectories. For practical purposes we took λ to be zero, whenever it was less than 0.001. In fact, we found that λ was either a positive quantity significantly (a few orders of magnitude) larger than 0.001, corresponding to chaotic trajectories, or a number less than 0.001, corresponding to regular trajectories.

The sectional curvature $K^{(2)}$ corresponding to CQO is given by

$$K^{(2)}_{CQO}=\frac{1}{p_1^2+p_2^2}[(12q_1^2+2\alpha q_2^2)p_2^2+(12q_2^2+2\alpha q_1^2)p_1^2 -8\alpha q_1 q_2 p_1 p_2]. \tag{20}$$

For this system, we compute $\langle K^{(2)}_{-}\rangle$ using Eqs. (16), (17), and (20). The maximal Lyapunov exponent λ is computed for $E=1024$ and several values of α. λ is computed for 2000 random initial conditions for each value of α corresponding to this energy. From this, we find $\langle\lambda\rangle$, the average value of the Lyapunov exponent and f over the 2000 initial conditions for a particular value of α. $\langle\lambda\rangle$ and f differ very little from their values corresponding to 500 or 1000 random initial conditions indicating that the size of the sample chosen for computations is more than adequate. To facilitate

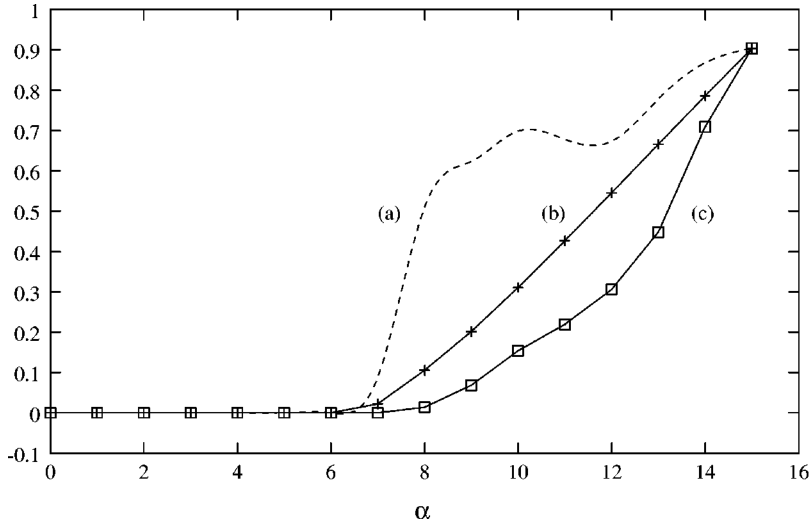

FIG. 2. Plots of (a) *f*, (b) $-0.1533\ \langle K_-^{(2)}\rangle$, and (c) $0.1012\ \langle\lambda\rangle^2$ against α for the system of coupled quartic oscillators.

comparison among $\langle K_-^{(2)}\rangle$, f, and $\langle\lambda\rangle^2$, we plot them in the same graph against α in Fig. 2. $\langle K_-^{(2)}\rangle$ and $\langle\lambda\rangle^2$ are normalized such that at $\alpha=15$, the scaled values of $\langle K_-^{(2)}\rangle$ and $\langle\lambda\rangle^2$ are equal to $f(=0.904)$ at $\alpha=15$. It is seen that $\langle K_-^{(2)}\rangle$ is closely related to $\langle\lambda\rangle^2$ rather than *f*. We will discuss this point later.

It is remarkable that all the quantities are zero for $\alpha<6$. This can be understood from the stability analysis of the system or the Toda-Brumer criterion [9,12]. The equation of motion for a conservative system with potential $V(q_i)$ is given by

$$\frac{d^2q_i}{dt^2}=-\frac{\partial V}{\partial q_i},\quad i=1,\ 2. \tag{21}$$

The stability of a trajectory is determined by considering infinitesimal variations δq_i of q_i, which satisfy the equations,

$$\frac{d^2\delta q_i}{dt^2}=-W_{ij}\delta q_j, \tag{22}$$

where

$$W_{ij}=\frac{\partial^2 V}{\partial q_i\partial q_j}, \tag{23}$$

is the *stability matrix*. By a suitable orthogonal transformation Ω,

$$\xi_k=\Omega_{ki}\delta q_i, \tag{24}$$

we can diagonalize $W=\partial_q^2V$. The eigenvalues σ_1, σ_2 of W are given by

$$\sigma_{1,2}=\tfrac{1}{2}\left[r+t\pm\sqrt{(r+t)^2-4(rt-s^2)}\right], \tag{25}$$

where

$$r=\frac{\partial^2V}{\partial q_1^2},\quad t=\frac{\partial^2V}{\partial q_2^2},\quad \text{and}\quad s=\frac{\partial^2V}{\partial q_1\partial q_2}. \tag{26}$$

In the diagonal representation,

$$\frac{d^2\xi_k}{dt^2}=-\sigma_k\xi_k, \tag{27}$$

whose solution is

$$\xi_k(t)=\exp(\sqrt{-\sigma_k}t)\xi_k(0). \tag{28}$$

If we have a region where $rt-s^2=\det[\partial_q^2V]$ is negative, then one of the eigenvalues σ_1 or σ_2 is necessarily negative and for this negative eigenvalue, ξ or δq evolves exponentially with time. Hence, the system is hyperbolic, corresponding to diverging trajectories, when $\det[\partial_q^2V]<0$.

For the coupled quartic oscillator, $V=q_1^4+q_2^4+\alpha q_1^2q_2^2$ and this translates into the inequality,

$$(\alpha-6)(\alpha+2)q_1^2q_2^2-2\alpha(q_1^2-q_2^2)^2>0. \tag{29}$$

As α is positive, this inequality is satisfied only when $\alpha>6$. When $\alpha<6$, $rt-s^2>0$ for all values of q_1 and q_2. Then $(r+t)^2-4(rt-s^2)=(r-t)^2+4s^2$ is positive and less than $(r+t)^2$. Hence σ_1 and σ_2 are necessarily real and positive. As a consequence, there are no diverging or chaotic trajectories when $\alpha<6$.

From Eqs. (18) and (20), it is easily seen that under the scaling transformation, $p_i\to\beta^{1/2}p_i$, $q_i\to\beta^{1/4}q_i$, the energy scales as $E\to\beta E$ and $K^{(2)}$ scales as $K^{(2)}\to\beta^{1/2}K^{(2)}$. Hence $\langle K_-^{(2)}\rangle$ scales as $\langle K_-^{(2)}\rangle\sim E^{1/2}$ when the energy is varied. Under the same scaling transformation, $\partial_q^2V\to\beta^{1/2}\partial_q^2V$, as V is a homogeneous quartic in q_1 and q_2. The eigenvalues of the stability equation, σ_i have the same scaling property as ∂_q^2V. Hence $\sigma_i\to\beta^{1/2}\sigma_i$, under this transformation. The Lyapunov exponent λ is the average exponential rate of divergence of neighboring trajectories. From Eq. (28) it is clear that $\lambda\sim\sqrt{-\sigma_k}$ as far as the scaling properties are concerned, though λ is a global quantity and σ_k are local by nature. This

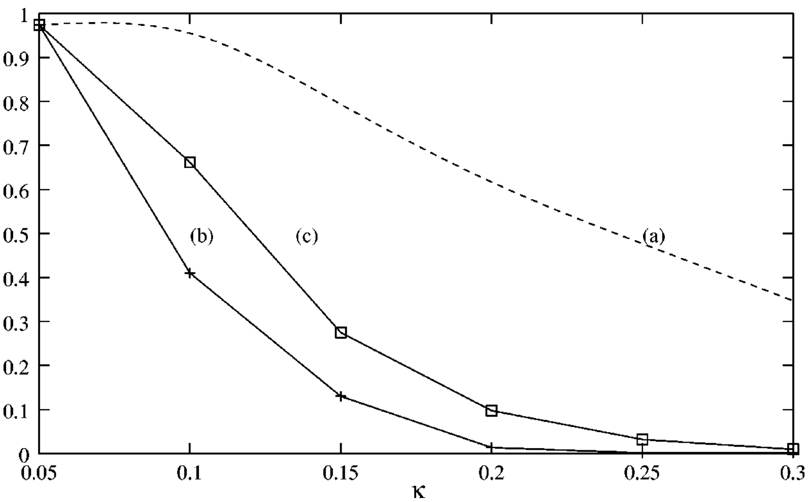

FIG. 3. Plots of (a) f, (b) $-3.943\ \langle K_-^{(2)}\rangle$, and (c) $0.648\ \langle\lambda\rangle^2$ against κ for the Yang-Mills-Higgs system.

implies that $\lambda\rightarrow\beta^{1/4}\lambda$ under the scaling transformation. Hence $\lambda\sim E^{1/4}$ when the energy is varied. Obviously, the scaling property is valid for any value of energy.

Our numerical data confirm these scaling relations, as well as the fact that the fraction of phase space f corresponding to chaotic trajectories does not vary with E for a given α. This is the reason why $\langle K_-^{(2)}\rangle$ has close correspondence with $\langle\lambda\rangle^2$, rather than with f.

For the YMH system described by the Hamiltonian in equation (19), $K^{(2)}$ is given by

$$K_{YMH}^{(2)}=\frac{1}{p_1^2+p_2^2}[(9q_1^2+6q_2^2)p_2^2+(6q_1^2+18\kappa q_2^2-\kappa)p_1^2 -24q_1q_2p_1p_2]. \tag{30}$$

We compute $\langle K_-^{(2)}\rangle$ using Eqs. (16), (17), and (23) and the maximal Lyapunov exponent λ for various values of κ and $E=100$. λ is computed for 2000 random initial conditions corresponding to this energy. For this we find $\langle\lambda\rangle$, the average value of Lyapunov exponent and f, the fraction of phase space corresponding to chaotic trajectories, for various values of κ. We explicitly checked out that $\langle\lambda\rangle$ and f did not vary when different sets of 2000 random initial conditions were used. In Fig. 3, we plot $\langle K_-^{(2)}\rangle$, f, and $\langle\lambda\rangle^2$ vs κ. Here again $\langle K_-^{(2)}\rangle$ and $\langle\lambda\rangle^2$ are reasonably close to each other (apart from a scale factor), whereas there is marked difference between the behavior of $\langle K_-^{(2)}\rangle$ and f. $\langle K_-^{(2)}\rangle$ is very close to zero around $\kappa=0.25$, whereas $f\approx0.2$ even at $\kappa=0.4$. In fact, corresponding to this value of κ, λ for the chaotic trajectories is ≈0.14. In an earlier work on the onset of chaos in this model, Kawabe [11] had reported the transition from mostly regular motion at large values of κ to almost totally stochastic motion at small values of κ with the coexistence of invariant curves and stochastic orbits at $\kappa\approx0.4$. Our numerical results are in agreement with his studies.

Though the value $\kappa\approx0.25$ for transition from chaos to order, estimated from the behavior of $\langle K_-^{(2)}\rangle$ is low, it is close to the value determined by the Toda-Brumer stability condition $\det(\partial_q^2V)<0$. We obtain the following inequality for diverging trajectories:

$$(2q_2^2+3q_1^2)\left(2q_1^2+6\kappa q_2^2-\frac{\kappa}{3}\right)-16q_1^2q_2^2<0. \tag{31}$$

It is not straightforward to obtain a clear-cut criterion for chaos from this inequality [10]. This is due to the fact that the potential is not homogeneous and contains a quadratic term also, apart from the quartic terms. However, if we ignore the quadratic term, the stability condition yields

$$q_1^4+(3\kappa-2)q_1^2q_2^2+2\kappa q_2^4<0,$$

or

$$\left[x^2+\frac{(3\kappa-2)}{2\kappa}x+\frac{1}{2\kappa}\right]<0, \tag{32}$$

where $x=q_2^2/q_1^2$. This can be satisfied only if both the roots of the quadratic form are real, leading to the relation

$$(3\kappa-2)^2-8\kappa>0,$$

or

$$(3\kappa-6)\left(3\kappa-\frac{2}{3}\right)>0. \tag{33}$$

This implies that $\kappa<\frac{2}{9}$ or $\kappa>2$. However, the system is definitely chaotic for low values of κ. Hence, $\kappa=\frac{2}{9}\approx0.22$ is the estimate for the critical value associated with order-chaos transitions from stability considerations. This is close to the value estimated by computing $\langle K_-^{(2)}\rangle$.

Next, we consider the variation of $\langle K_-^{(2)}\rangle$, f and $\langle\lambda\rangle^2$ with energy E. In Fig. 4, we plot $\log_2\langle K_-^{(2)}\rangle$, f and $\log_2\langle\lambda\rangle^2$ against $\log_2 E$ for $\kappa=0.1$. f is a constant at high energies. Even at lower energies, there is very little variation in f. The slopes of the log-log plots of both $\langle K_-^{(2)}\rangle$ and $\langle\lambda\rangle^2$ are very close to 0.5, indicating that both these quantities scale as $E^{1/2}$. As we pointed out earlier, this is expected for a homo-

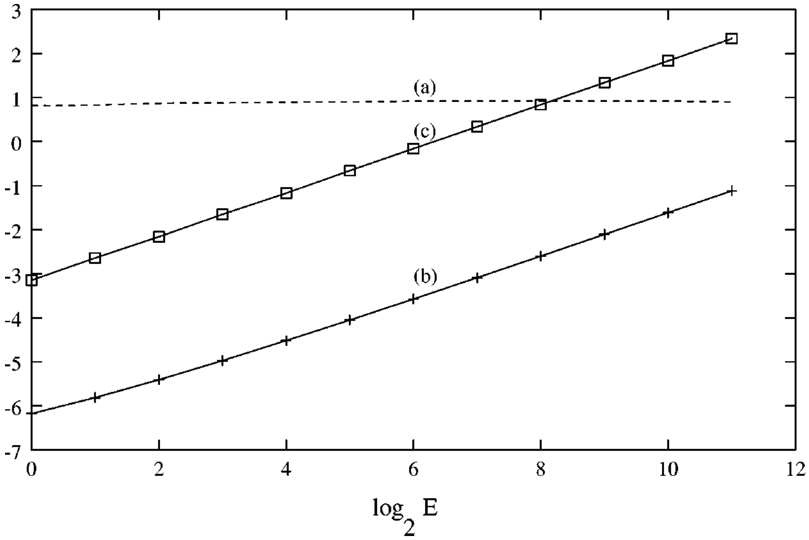

FIG. 4. Plots of (a) f, (b) $\log_2(-\langle K_-^{(2)}\rangle)$, and (c) $\log_2(\langle\lambda\rangle^2)$ against $\log_2 E$ for the Yang-Mills-Higgs system with $\kappa=0.1$.

geneous quartic potential. It is remarkable that it is true even for the model under consideration, though the potential contains a quadratic term.

III. CONCLUSIONS

A recently proposed geometric description of Hamiltonian chaos has been very successful, both in qualitative and quantitative aspects. For systems with a large number of degrees of freedom, it even provides an analytic estimate of the maximal Lyapunov exponent, without having to solve equations of motion and the tangent dynamics. For systems with a small number of degrees of freedom, it has been claimed that $\langle K_-^{(2)}\rangle$ (a suitably defined sectional curvature averaged over its negative values over a constant energy manifold), is an indicator of the global degree of chaoticity at that energy. We have investigated in detail, the relations among $\langle K_-^{(2)}\rangle$, the average maximal Lyapunov exponent $\langle\lambda\rangle$ at a given energy, and the fraction of phase space f corresponding to chaotic trajectories, for two systems of physical interest. We find that $\langle K_-^{(2)}\rangle$ is closely related to $\langle\lambda\rangle^2$, rather than to f, in contrast to what the previous work seems to imply. Both $\langle K_-^{(2)}\rangle$ and $\langle\lambda\rangle^2$ scale as $E^{1/2}$, for the quartic potentials we have considered. In fact, for potentials that are of nth degree in the coordinates, it is easy to see that both $\langle K_-^{(2)}\rangle$ and $\langle\lambda\rangle^2$ scale as $E^{(n-2)/n}$. Thus the linear relation between $\langle K_-^{(2)}\rangle$ and $\langle\lambda\rangle^2$ is expected to be a general feature of Hamiltonian systems. However, there are some issues which require a more detailed study. For instance, we noted that the critical value of κ associated with the transition from chaos to order in the Yang-Mills-Higgs system estimated from $\langle K_-^{(2)}\rangle$, was lower than the estimate provided by f and the Poincaré sections. Thus there is need for finding a geometrical entity that can explain order chaos transitions more accurately.

ACKNOWLEDGMENT

One of the authors (K.R.) thanks the Council of Scientific and Industrial Research, India for financial support.

[1] M. Pettini, Phys. Rev. E **47**, 828 (1993).
[2] L. Casetti and M. Pettini, Phys. Rev. E **48**, 4320 (1993).
[3] L. Casetti, R. Livi, and M. Pettini, Phys. Rev. Lett. **74**, 375 (1995).
[4] M. Cerruti-Sola and M. Pettini, Phys. Rev. E **53**, 179 (1996).
[5] L. Casetti, M. Pettini, and E. G. D. Cohen, Phys. Rep. **337**, 237 (2000).
[6] T. Levi-Civita, Ann. Math. **97**, 291 (1926).
[7] P. Cipriani and M. Di Bari, Phys. Rev. Lett. **81**, 5532 (1998).
[8] L. P. Eisenhart, Ann. Math. **30**, 591 (1929).
[9] T. S. Biro, S. G. Matinyan, and B. Muller, *Chaos and Gauge Field Theory* (World Scientific, Singapore, 1994).
[10] C. N. Kumar and A. Khare, J. Phys. A **22**, L849 (1989).
[11] T. Kawabe, Phys. Lett. B **274**, 399 (1992).
[12] M. Toda, Phys. Lett. A **48**, 335 (1974); P. Brumer and W. Duff, J. Chem. Phys. **65**, 3566 (1976).